

# PREDICTION OF SLURRY PUMP COMPONENT WEAR AND COST

A. Sellgren<sup>1</sup>, G. Addie<sup>2</sup>, R. Visintainer<sup>3</sup> and K. Pagalthivarthi<sup>4</sup>

## ABSTRACT

Slurry pumps are used for the transportation of solids in coal, copper, iron ore, phosphate and in other mining operations. They are also used on dredges cleaning waterways, in environmental cleanup and in reclaiming land throughout the world.

Slurries by their very nature are very abrasive requiring the impeller, casing and suction liner wet end component parts be replaced at regular intervals. It is not uncommon, for example, for six liners, three impellers and two casings to be consumed in one year. It is estimated that about \$500 million in slurry pump wear parts are consumed every year.

Numerical models now exist to predict component wear for a given set of operating conditions with a given design. The use of these models is however available to a select few and no general relations exist for the user.

The writers in this paper model a selection of pump designs producing general relationships for the different pump casing, impeller and liner components for different duties. They then take these and show which offer the lowest cost of ownership for different services.

**Keywords:** Slurry Transport, Wear Rate, CFD Simulation, Lowest Cost of Ownership

## INTRODUCTION

In this study, existing numerical flow simulation methods have been applied to a broad range of slurry pump designs and sizes at various operating conditions including ranges of flow, head, solids size and solids concentration. The resulting data were then analyzed for significant trends and are reported here in some detail.

These results show that many of the variables considered can have dramatic effects on the pump wear rates and therefore also on the costs of system operation, both from the viewpoint of component replacement, as well as downtime associated with pump repairs. Seemingly simple changes such as adding or removing one pump from a long pipeline, or pumping at a slightly different concentration, can easily double or halve the life of the wear parts.

The goals of this study have been several:

1. To quantify the effects of important slurry pump operating parameters and design geometries on component wear.
2. To investigate the overall cost of operating a slurry pump relative to the operating conditions and design types.
3. To provide a guide for determining what design type of slurry pump is best suited for each application.
4. To provide the pump user with generic tools for determining slurry pump wear rates and costs during the planning stages of slurry system design.

It is hoped that the data presented here will provide designers and users alike a better understanding of slurry pump wear behavior and how this critical component in many mining and dredging operations can be more effectively utilized.

---

<sup>1</sup> Prof., Lulea University of Technology, Lulea, Sweden

<sup>2</sup> V.P. Engineering, Research and Development, GIW Industries Inc., Grovetown, GA, USA

<sup>3</sup> Chief Engineer, GIW Industries Inc., Grovetown, GA, USA

<sup>4</sup> Prof., Dept. of Applied Mechanics, Indian Institute of Technology, New Delhi, India

## Specific Speed

At any given rotational speed (rpm), every centrifugal pump has a particular flowrate where the efficiency is at a maximum. Ideally, the operating duty flowrate should be near this best efficiency (BEPQ) flow. The total dynamic head at this rpm and BEPQ is called the best efficiency (BEPH) head.

The specific speed ( $N_s$ ) is a type number that can be used to categorize different designs of pumps and is defined as:

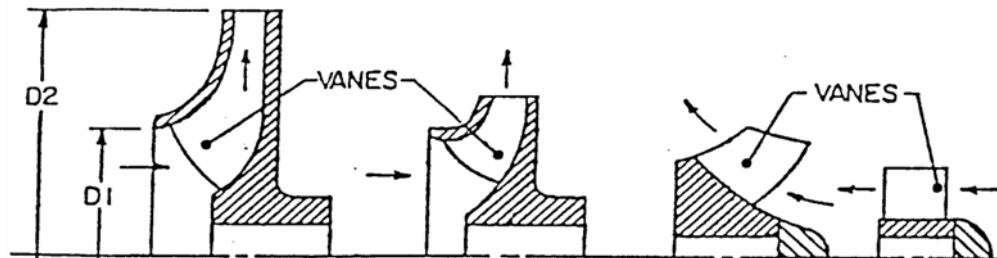
$$N_s = \frac{RPM \times \sqrt{BEPQ}}{BEPH^{3/4}} \quad (1)$$

Where:

BEPQ = m<sup>3</sup>/sec or USGPM

BEPH = m or ft.

Pumps of different specific speed can do the same duty at the best efficiency, but a lower specific speed pump will have a bigger impeller and run slower than a higher specific speed pump. Typical impellers of different specific speeds are shown in Figure 1.



	Units	Centrifugal Single Suction	Mixed Flow Single Suction	Mixed Flow Propeller	Axial Flow Propeller
$N_s$	metric (US)	35 (1800)	60 (3000)	120 (6250)	265 (13500)
Flow	m <sup>3</sup> /hr (gpm)	550 (2400)	550 (2400)	550 (2400)	550 (2400)
Head	m (ft)	21 (70)	15 (50)	10 (33)	6 (20)
Rpm	(-)	870	1160	1750	2600
D2	mm (in)	483 (19)	305 (12)	254 (10)	178 (7)
D1/D2	(-)	0.5	0.7	0.9	1.0

**Figure 1. Impellers of Different Specific Speeds with Representative Operating Conditions.**

## Numerical Modelling of Flow and Wear

The wear in a slurry pump usually refers to the wear of the main wetted components: the casing, the impeller and the suction liner as shown in Figure 2. The wear distribution in these parts is usually uneven, therefore, a limiting wear life is determined based on the time taken to wear through a nominated percentage of the component thickness at the location of maximum wear.

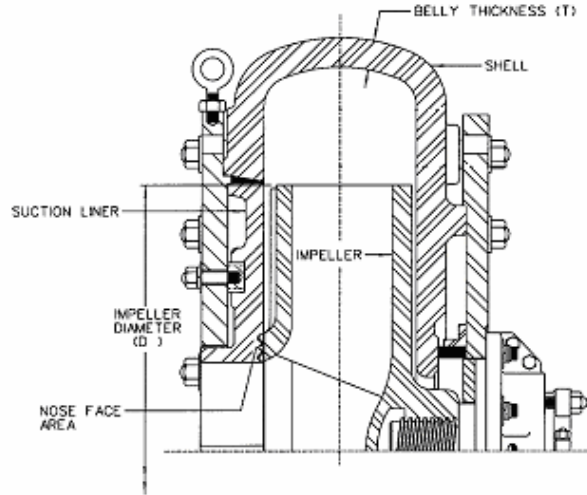


**Figure 2. Cross Section of a Typical Slurry Pump.**

The availability of high-speed computers with ample memory has encouraged many researchers to develop numerical algorithms for analysing the flow, and resulting wear, in pumps and other components of slurry pipeline systems. Since wear depends on local values of velocity and concentration, the flow and concentration fields must be computed prior to wear evaluation. Numerical simulation of fluid and particulate flow involves transformation of the governing partial differential equations of fluid and particle motion into non-linear algebraic equations which are solved by an iterative algorithm relative to the boundary conditions (i.e. the inlet flow, outlet flow and pump geometry). The generic term for this approach is Computational Fluid Dynamics (CFD). Once determined, the flow field velocities and concentrations may be used to determine the wear rate via correlations between the energy expended at the wearing surface and the amount of material removed. These correlations are determined by specially designed laboratory experiments. A number of commercially available CFD programs exist, but those for dense solid-liquid mixtures (slurries) are generally proprietary.

One of the major advantages of numerical analysis is that once a general algorithm has been developed and validated, solutions are easily generated for a wide range of geometries, whereas multiple physical experiments can be prohibitively expensive. In a conceptual sense, the numerical analyst 'turns on' the algorithm and awaits results, just as the physical experimenter starts an experiment and then observes what happens. The numerical analyst has the advantage of being able to alter the variables which represent material properties and boundary conditions, and the ability to test the sensitivity of the studied phenomena to various assumptions or constraints.

In the present study, some parameters have been held fixed to bring the number of variables within reasonable limits. In particular, the wear correlation parameters are for a silica sand slurry of typical size distribution ( $D_{85} = 2.3 \times D_{50}$ ) against high chrome white iron slurry pump components. All of the pumps are running at, or near, their design flowrates.

The numerical models themselves are described in (Roco et. al. 1983, 1984) and (Pagalthivartha et. al 2004, 1992,1991) for the casing wear, (Bross et. al. 2001) for the suction liner wear and (Pagalthivartha et. al. 2001) for the impeller wear. The experiments used to validate the code are shown in (Kadambi et al, 2003) and the wear correlations are described in (Tian, 2003).

### **Pump Data for this Study**

The dimensional and performance data for this study came from pumps designed, manufactured and tested at GIW Industries over the last 25 years. Pumps were selected in four different size groups with best efficiency (BEPQ) flowrates near 11400, 8000, 5700 and 2300 m<sup>3</sup>/hr (50000, 35000, 25000 and 10000 gpm) while producing approximately 50m (164 ft) of head. A special fifth group of high specific speed designs covering a range of sizes was also selected because these design are less common and were not widely represented in the other groups. Tables 1 and 2 list the characteristic dimensions and operating conditions for each of the pumps used in this study.

**Table 1. The Study Pumps: Branch and Impeller Dimensions.**

No.	Designation	Discharge Diameter		Suction Diameter		Impeller Diameter		No. of Vanes	Vane Sweep deg.	Impeller Outlet Width		Adj. Clearing Vane Depth	
		mm	(in)	mm	(in)	mm	(in)			mm	(in)	mm	(in)
1	LSA 36	254	(10)	305	(12)	914	(36.0)	3	125	171	(6.8)	7.6	(0.30)
2	LSA 32	254	(10)	305	(12)	813	(32.0)	3	126	171	(6.8)	6.7	(0.26)
3	LCC 26	254	(10)	305	(12)	660	(26.0)	3	130	143	(5.6)	5.5	(0.22)
4	LHD 22	305	(12)	305	(12)	559	(22.0)	3	90	203	(8.0)	4.6	(0.18)
5	LCC28	305	(12)	356	(14)	710	(28.0)	3	130	162	(6.4)	5.9	(0.23)
6	PTA 25	305	(12)	356	(14)	641	(25.3)	4	93	148	(5.8)	5.3	(0.21)
7	LSA 62	406	(16)	533	(21)	1575	(62.0)	3	112	318	(12.5)	13.0	(0.51)
8	WBC 54	457	(18)	508	(20)	1372	(54.0)	3	135	203	(8.0)	11.4	(0.45)
9	LSA 52	457	(18)	508	(20)	1321	(52.0)	3	127	227	(8.9)	10.9	(0.43)
10	LSA 44	457	(18)	457	(18)	1118	(44.0)	3	120	295	(11.6)	9.3	(0.36)
11	LHD 33	457	(18)	457	(18)	838	(33.0)	3	115	203	(8.0)	6.9	(0.27)
12	LHD 31	457	(18)	457	(18)	787	(31.0)	3	111	203	(8.0)	6.5	(0.26)
13	LHD 27	457	(18)	457	(18)	686	(27.0)	3	110	147	(5.8)	5.7	(0.22)
14	LHD 42	559	(22)	610	(24)	1067	(42.0)	3	92	306	(12.0)	8.8	(0.35)
15	LHD 44	610	(24)	610	(24)	1118	(44.0)	3	88	406	(16.0)	9.3	(0.36)
16	LSA 48	508	(20)	610	(24)	1219	(48.0)	3	129	229	(9.0)	10.1	(0.40)
17	LSA 54	559	(22)	610	(24)	1372	(54.0)	4	100	343	(13.5)	11.4	(0.45)
18	TBC 57.5	610	(24)	610	(24)	1435	(56.5)	4	131	295	(11.6)	11.9	(0.47)
19	HPD 62	508	(20)	610	(24)	1575	(62.0)	3	130	298	(11.8)	13.0	(0.51)
20	HHD 73	508	(20)	610	(24)	1930	(76.0)	4	93	391	(15.4)	16.0	(0.63)
21	HPD 91	813	(32)	914	(36)	2311	(91.0)	3	148	400	(15.8)	19.1	(0.75)
22	TBC 84	762	(30)	864	(34)	2134	(84.0)	3	145	375	(14.8)	17.7	(0.70)
23	HHD 80	686	(27)	737	(29)	2032	(80.0)	3	127	470	(18.5)	16.8	(0.66)
24	HHD 76	610	(24)	660	(26)	1930	(76.0)	3	140	337	(13.3)	16.0	(0.63)
25	WBC 68	711	(28)	711	(28)	1727	(68.0)	5	95	318	(12.5)	14.3	(0.56)
26	TBC 64	660	(26)	711	(28)	1702	(67.0)	3	126	344	(13.5)	14.1	(0.55)
27	MHD 60	660	(26)	660	(26)	1524	(60.0)	3	110	351	(13.8)	12.6	(0.50)
28	LSA 58	660	(26)	711	(28)	1464	(57.6)	4	100	298	(11.8)	12.1	(0.48)
29	LHD 50	660	(26)	711	(28)	1270	(50.0)	3	118	302	(11.9)	10.5	(0.41)
30	LHD 49	610	(24)	660	(26)	1261	(49.6)	4	104	358	(14.1)	10.4	(0.41)
31	FGD 44	610	(24)	610	(24)	1118	(44.0)	5	88	264	(10.4)	9.3	(0.36)
32	LHD 44	610	(24)	610	(24)	1113	(43.8)	3	88	406	(16.0)	9.2	(0.36)
33	FGD 43	762	(30)	762	(30)	1110	(43.7)	5	90	260	(10.2)	9.2	(0.36)
34	LHD 43(46)	762	(30)	762	(30)	1168	(46.0)	4	103	203	(8.0)	9.7	(0.38)
35	LHD 44	508	(20)	610	(24)	1113	(43.8)	3	92	406	(16.0)	9.2	(0.36)
36	LHD 33	457	(18)	457	(18)	841	(33.1)	2	142	203	(8.0)	7.0	(0.27)
37	LHD 43	762	(30)	762	(30)	1097	(43.2)	5	88	260	(10.2)	9.1	(0.36)
38	LHD 43(40)	762	(30)	762	(30)	1016	(40.0)	5	88	260	(10.2)	8.4	(0.33)
39	LHD 43(38)	762	(30)	762	(30)	971	(38.2)	5	88	260	(10.2)	8.0	(0.32)
40	LHD 43	762	(30)	762	(30)	1097	(43.2)	5	88	260	(10.2)	9.1	(0.36)
41	FGD 45	914	(36)	914	(36)	1143	(45.0)	5	85	325	(12.8)	9.5	(0.37)

**Table 2. The Study Pumps: Operating Conditions and Casing Dimensions.**

No.	Designation	Pump Specific Speed		Flowrate		RPM @50m TDH	BEPQ %	Casing Throat Radius		Casing Inside Width	
		metric	(US)	m <sup>3</sup> /hr	(usgpm)			mm	(in)	mm	(in)
1	LSA 36	24.8	(1283)	2271	(10000)	648	108	670	(26.4)	262	(10.3)
2	LSA 32	25.3	(1306)	2271	(10000)	777	129	632	(24.9)	262	(10.3)
3	LCC 26	29.2	(1508)	2271	(10000)	990	141	505	(19.9)	203	(8.0)
4	LHD 22	56.3	(2911)	2271	(10000)	1134	72	578	(22.8)	264	(10.4)
5	LCC28	36.4	(1879)	2271	(10000)	876	98	650	(25.6)	279	(11.0)
6	PTA 25	38.7	(2002)	2271	(10000)	1001	103	580	(22.8)	226	(8.9)
7	LSA 62	26.6	(1373)	5678	(25000)	373	88	1173	(46.2)	417	(16.4)
8	WBC 54	27.0	(1397)	5678	(25000)	440	107	1107	(43.6)	356	(14.0)
9	LSA 52	26.2	(1352)	5678	(25000)	460	117	1092	(43.0)	406	(16.0)
10	LSA 44	32.6	(1684)	5678	(25000)	548	110	906	(35.7)	406	(16.0)
11	LHD 33	50.3	(2602)	5678	(25000)	811	103	886	(34.9)	292	(11.5)
12	LHD 31	56.1	(2897)	5678	(25000)	858	97	839	(33.0)	292	(11.5)
13	LHD 27	71.9	(3716)	5678	(25000)	1243	107	870	(34.3)	267	(10.5)
14	LHD 42	56.5	(2921)	7949	(35000)	618	80	965	(38.0)	439	(17.3)
15	LHD 44	58.9	(3042)	7949	(35000)	553	61	1149	(45.3)	526	(20.7)
16	LSA 48	38.6	(1997)	7949	(35000)	529	105	1035	(40.8)	457	(18.0)
17	LSA 54	33.1	(1710)	7949	(35000)	413	95	1003	(39.5)	508	(20.0)
18	TBC 57.5	28.8	(1488)	7949	(35000)	401	109	1160	(45.7)	455	(17.9)
19	HPD 62	27.9	(1440)	7949	(35000)	378	106	1173	(46.2)	417	(16.4)
20	HHD 73	24.7	(1277)	7949	(35000)	322	101	1353	(53.3)	508	(20.0)
21	HPD 91	25.7	(1327)	11356	(50000)	248	87	1544	(60.8)	533	(21.0)
22	TBC 84	26.4	(1362)	11356	(50000)	271	93	1508	(59.4)	508	(20.0)
23	HHD 80	25.2	(1300)	11356	(50000)	288	108	1619	(63.8)	584	(23.0)
24	HHD 76	26.0	(1346)	11356	(50000)	309	112	1353	(53.3)	559	(22.0)
25	WBC 68	29.4	(1519)	11356	(50000)	364	116	1473	(58.0)	559	(22.0)
26	TBC 64	27.6	(1427)	11356	(50000)	338	117	1353	(53.3)	493	(19.4)
27	MHD 60	35.2	(1820)	11356	(50000)	400	105	1232	(48.5)	483	(19.0)
28	LSA 58	36.6	(1894)	11356	(50000)	420	106	1272	(50.1)	490	(19.3)
29	LHD 50	48.8	(2524)	11356	(50000)	535	100	1225	(48.2)	442	(17.4)
30	LHD 49	42.0	(2169)	11356	(50000)	488	108	1098	(43.2)	478	(18.8)
31	FGD 44	51.3	(2650)	11356	(50000)	593	106	1150	(45.3)	381	(15.0)
32	LHD 44	58.9	(3042)	11356	(50000)	571	84	1149	(45.3)	526	(20.7)
33	FGD 43	67.0	(3465)	11356	(50000)	581	76	1432	(56.4)	422	(16.6)
34	LHD 43(46)	60.9	(3147)	13008	(57275)	620	100	1433	(56.4)	422	(16.6)
35	LHD 44	62.6	(3234)	14309	(63001)	611	100	1149	(45.3)	526	(20.7)
36	LHD 33	62.8	(3246)	6019	(26500)	952	100	839	(33.0)	292	(11.5)
37	LHD 43	64.0	(3306)	15103	(66501)	607	100	1432	(56.4)	422	(16.6)
38	LHD 43(40)	76.1	(3933)	15785	(69501)	707	100	1432	(56.4)	422	(16.6)
39	LHD 43(38)	86.5	(4472)	16920	(74501)	771	100	1432	(56.4)	422	(16.6)
40	LHD 43	64.0	(3308)	15103	(66501)	613	100	1432	(56.4)	422	(16.6)
41	FGD 45	72.8	(3760)	20100	(88501)	601	100	1609	(63.3)	498	(19.6)

The pumps were selected to operate as close to the BEPQ as possible in each given flow range (or directly on the BEPQ in the case of the high specific speed pumps) at each of seven different combinations of head, volumetric solids concentration, and solids size as shown in Table 3 below. Case 1 from this table was considered the “baseline case” from which all of the other cases were derived by varying only one of the three variables at a time. Separate analyses were then run for the suction liners, casings and impellers. In total, about 800 separate analyses were run.

Case	Head m	Concentration Cv %	Solids Size D50 micron
1 (baseline)	50	20	300
2	35	20	300
3	65	20	300
4	50	10	300
5	50	40	300
6	50	20	150
7	50	20	600

Table 3. Variations of Head, Volumetric Concentration and Solids Size considered in this study.

## RESULTS OF THE NUMERICAL EXPERIMENTS

### Casing Wear

The casing wear rate considered in this study was the maximum wear in the two dimensional cross section along the casing radial centreline, or what is often termed the “belly” of the casing. Two dimensional, numeric CFD analyses were run for all of the pumps in the study at each of the seven sets of operating conditions. Example output for one such analysis is shown in Figure 3.

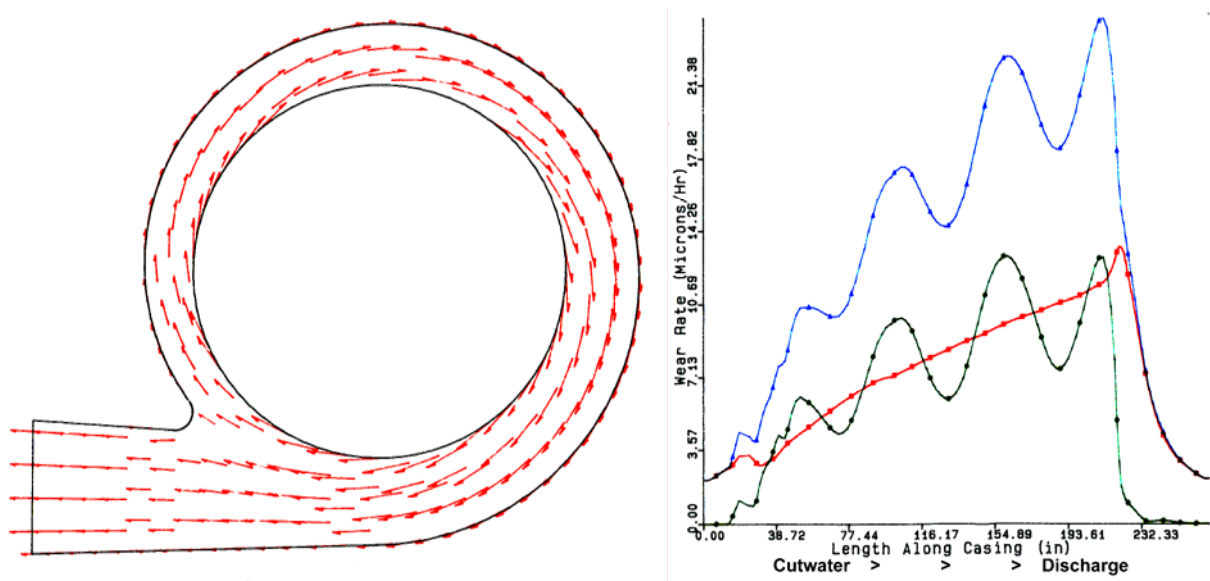


Figure 3. Example Output from 2D Casing Wear Numerical CFD analysis

The general results, relative to the pump specific speed ( $N_s$ ) are summarized by Figure 4, which shows a summary of the results for the baseline case (50 meter of head, 300 micron D50 solids size and 20% volumetric concentration). This plot shows a weak correlation of decreasing wear against increasing specific speed, which considering the differences in the geometry of the various pumps, is surprisingly good. More interesting perhaps is that the correlation appears to be independent of the size (flowrate) of the pumps.

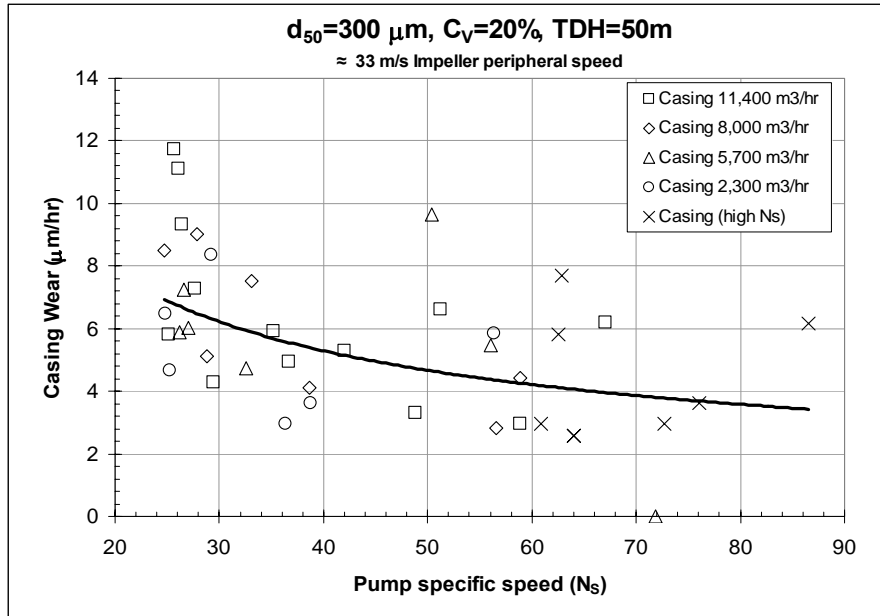


Figure 4. Casing Wear for the Baseline Case.

When taking the actual casing geometry into consideration, a better correlation can be found. In Figure 5, the wear is now plotted against the ratio ( $R_{T3} / D_2$ ) where  $D_2$  equals the impeller outer diameter and  $R_{T3}$  is the radius to the shell theoretical throat as shown. The same baseline case is considered. While there is some scatter among the higher specific speed pumps, a clear minimum trend is visible and the result is again independent of pump size.

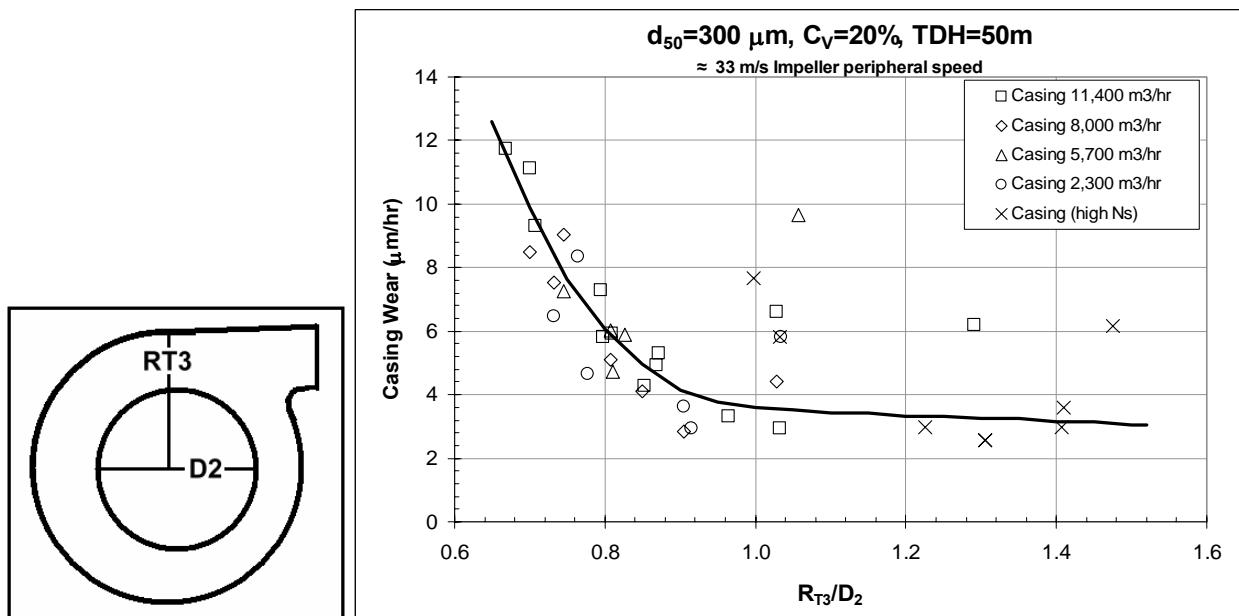
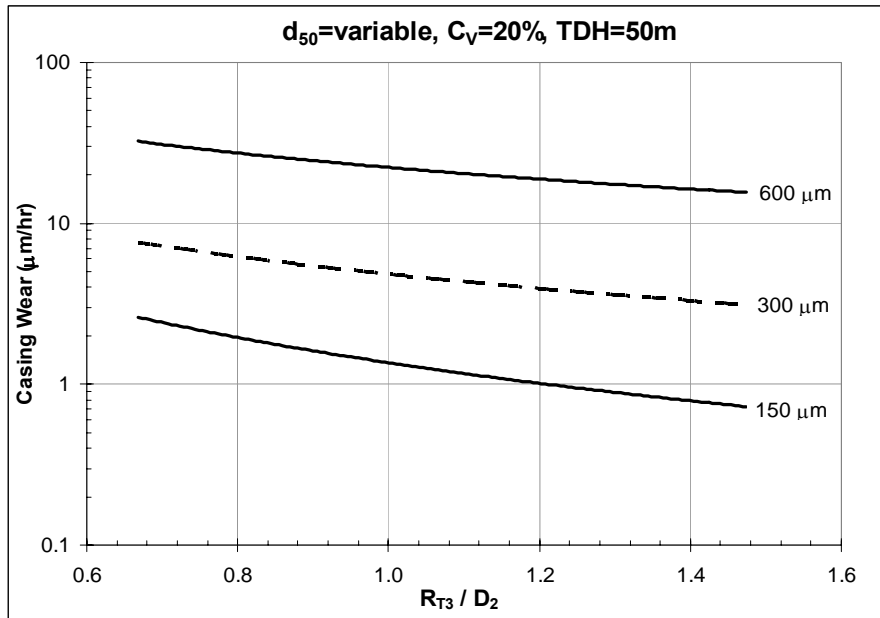


Figure 5. Correlation of Casing Wear to Design Geometry.

To give some appreciation for the effect that variations in the study parameters can have on the casing wear rate, Figure 6 shows the average trendlines for casing wear rate plotted against pump specific speed for a variation in  $D_{50}$  solids size from 150 microns to 600 microns. This four fold increase in solids size results in a twenty fold increase in the casing wear rate.



**Figure 6. Effect of Solids Size on Casing Wear Rate.**

### Suction Liner Wear

Next, suction liner wear rates were examined. In this case, the model is a theoretical / empirical formulation based on the geometry of the impeller / suction liner interface and the fluid equations of motion assuming an even pressure distribution within the casing. The rotation of the impeller clearing vanes sets up a rotation of the fluid that determines the pressure drop, and therefore flowrate and velocities, across the sealing gap. The wear rate is based on the resulting relative velocities between the impeller, liner and solids. Because actual liner wear is often uneven due to uneven casing pressure distributions and other factors, experience has shown that a multiplier of two should be applied to the results of this model, unless special balancing features are incorporated into the design. Figure 7 shows the key geometric parameters considered in this calculation.

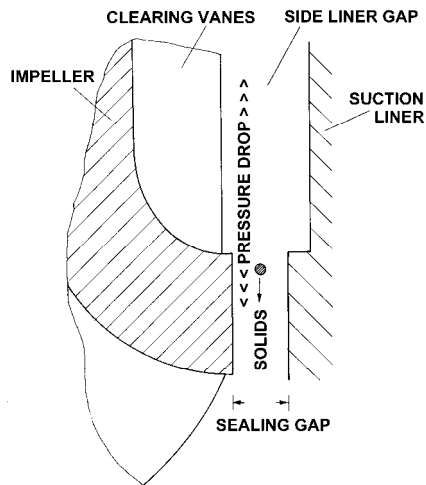


**Figure 7. Geometry used for Liner Wear Model**

Analyses were run for all of the pumps in the study at each of the seven sets of operating conditions, as was done with the casing. Representative of the results is Figure 8, where the correlation is both stronger than, and in the opposite direction to, that seen for the casing. It is also still independent of pump size.

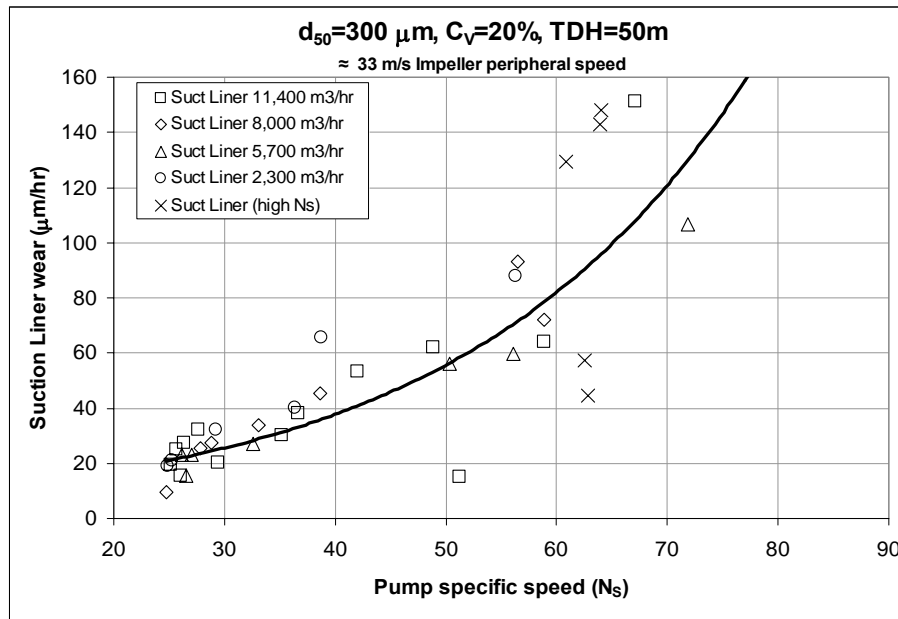


**Figure 8. Suction Liner Wear for the Baseline Case**

An even stronger correlation is seen when one considers the wear rate against the diameter ratio of the impeller outlet  $D_2$  over the inlet  $D_1$  as shown in Figure 9. Although this ratio itself correlates to pump specific speed, it is interesting to note that the wear in particular is even more strongly related to the geometry than to the pump design type.

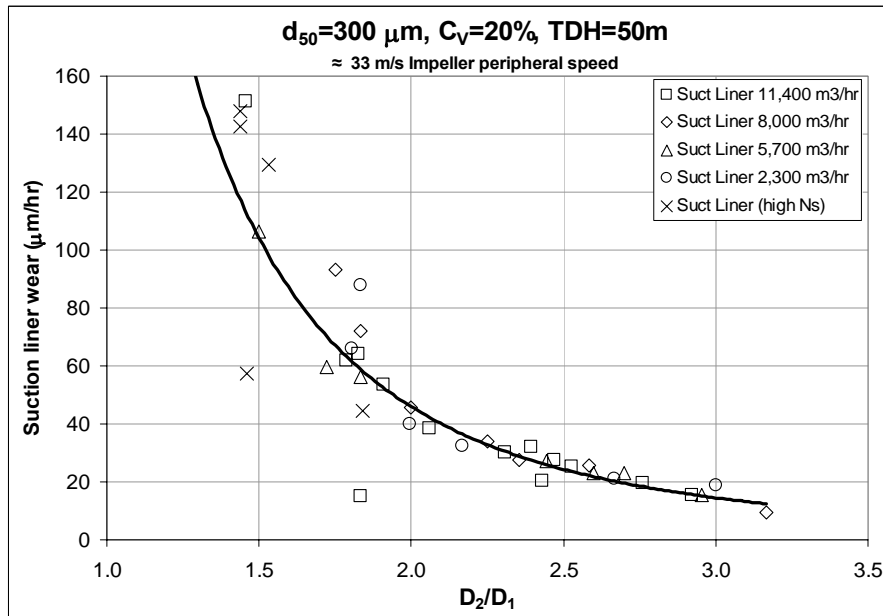


**Figure 9. Correlation of Suction Liner Wear to Design Geometry.**

To give some appreciation for the effect that variations in the study parameters can have on the liner wear rate, Figure 10 shows the trendlines for suction liner wear against the ( $D_2 / D_1$ ) ratio with a variation in pump head from 35m to 65m. The 85% increase in head results in a three fold increase in the liner wear rate.

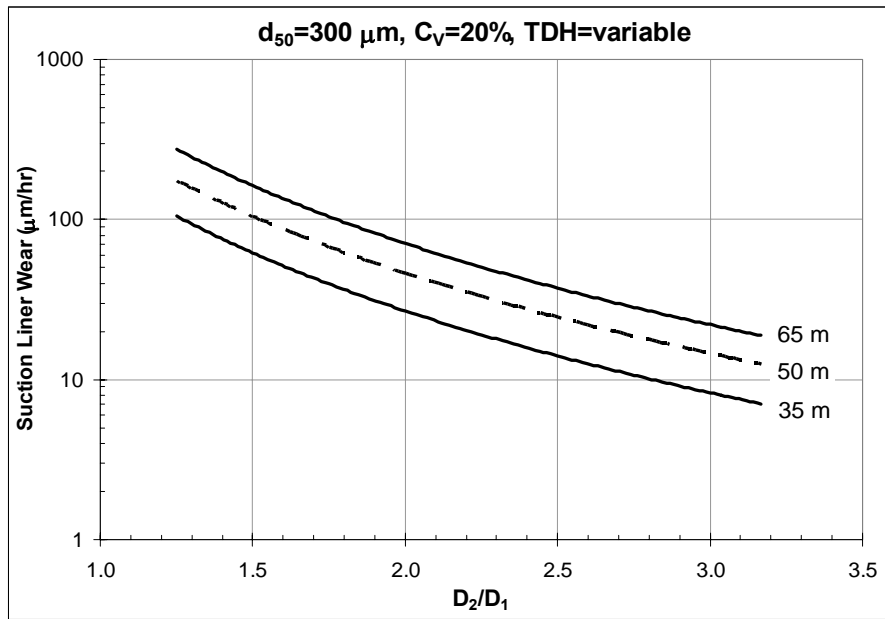


Figure 10. Effect of Pump Head on Liner Wear Rate.

### Impeller Wear

In the case of the impeller, a fully 3 dimensional, numerical CFD model was used and the wear rate considered was the average wear rate across both sides of the pumping vane. An example output for one such analysis is shown in Figure 11.

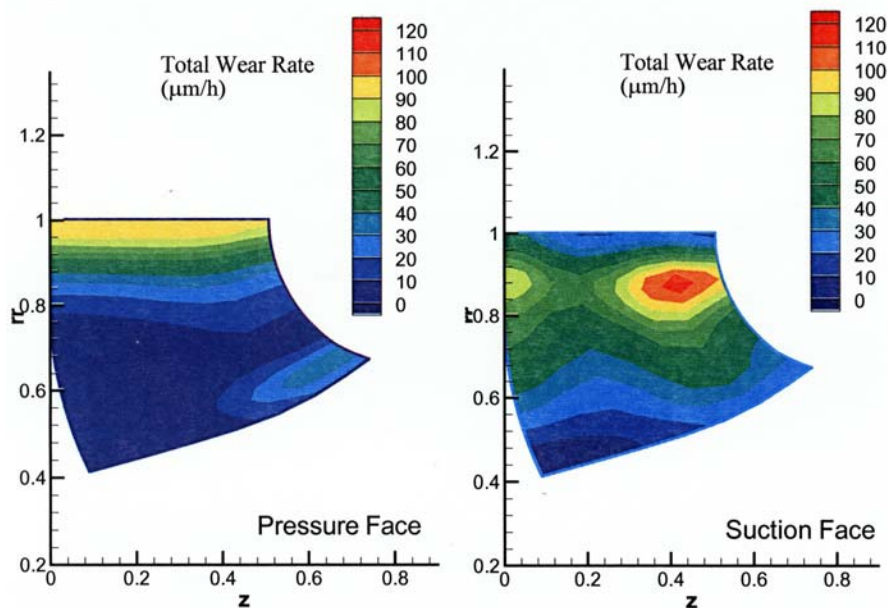


Figure 11. Example Output from 3D Impeller Wear Numerical CFD Analysis

Because of the relative difficulty in running fully 3D analyses, solutions were obtained for only 75% of the sample pumps for this part of the study. Once again, each design was run at each of the seven sets of operating conditions. Representative of the results is Figure 12, where a correlation to pump specific speed similar to that for the suction liner wear is evident.

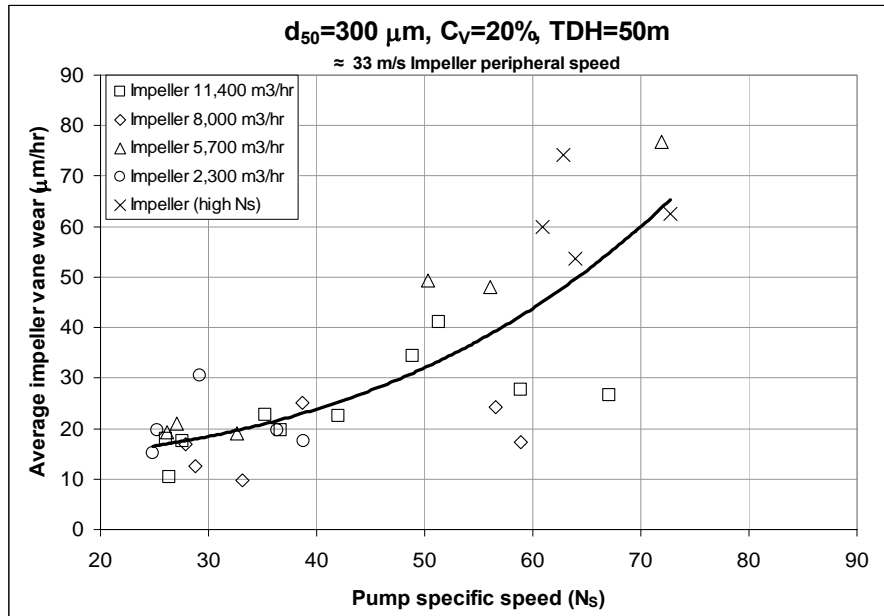


Figure 12. Average Impeller Vane Wear for the Baseline Case

An alternative correlation of wear against the ratio of the vane surface area to the impeller suction diameter squared ( $D_1^2$ ) is somewhat stronger as seen in Figure 13.

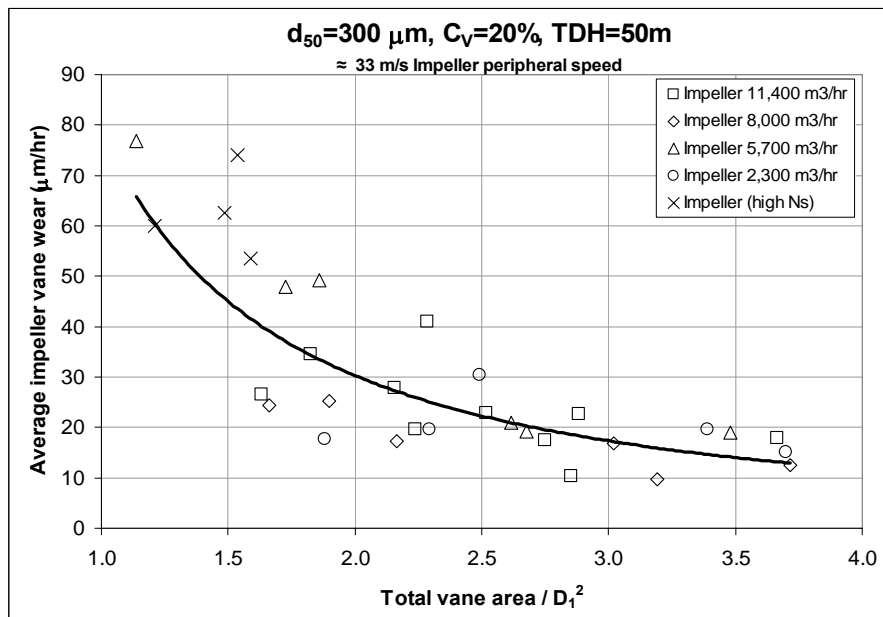


Figure 13. Correlation of Impeller Wear to Design Geometry.

To give some appreciation for the effect that variations in the study parameters can have on the impeller wear rate, Figure 14 shows trendlines for impeller wear against the ( $\text{Total Vane Area} / D_1^2$ ) ratio with a variation in volumetric slurry concentration from 10% to 40%. The four fold increase in concentration results in a ten fold

increase in the average impeller vane wear rate. It is also seen that the effect of concentration variations in the impeller are quite non-linear, indicating that the formation of a sliding bed of solids at the higher concentrations provides some protection against increasing wear with increases in concentration beyond 20%.

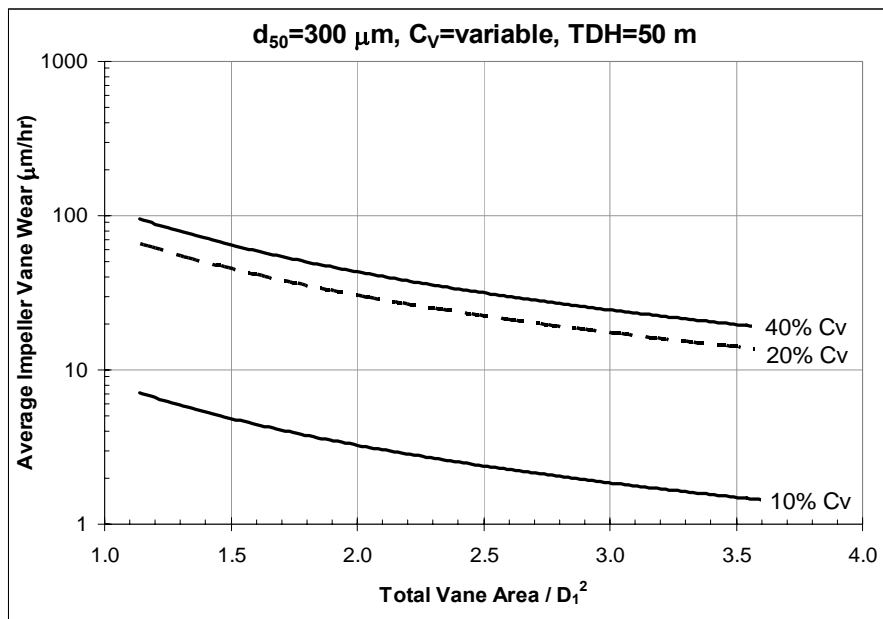


Figure 14. Effect of Slurry Volumetric Concentration on Impeller Wear Rate.

### SUMMARY OF AVERAGE WEAR RESULTS

It has not been possible to display all the graphs and correlations produced in this study. It was desired, however, to provide a summary that would quantify the most important trends and give the pump user a tool for estimating slurry pump component wear rates (suction liners, casings and impellers) based on the pump design type ( $N_s$ ),  $D_{50}$  solids size and slurry concentration. This summary is given in Figure 15 and is based on the trend line values for all of the pumps and seven duty conditions examined in this study.

To use Figure 15, first determine the specific speed of the slurry pump design in question. Using the closest specific speed in the figure, determine the baseline wear for each of the three components (suction liner, casing and impeller). Finally, make adjustments for deviations from the baseline case by interpolating along the given lines and determining the change in wear. Deviations in all three parameters can be considered in this way, and when taken as ratios of the baseline case, they can be combined into a single multiplier for calculation of the estimated wear rates.

Consider the following example

- Pump of specific speed ( $N_s$ ) = 25
- Pump head = 60 m
- $D_{50}$  solids size = 200  $\mu\text{m}$
- Volumetric solids concentration = 40%

From the suction liner chart for  $N_s = 25$ , the baseline case wear rate is about 20  $\mu\text{m}/\text{hour}$ . Reading from the variable head axis, the increase in head from the baseline of 50m to our actual 60 m increases the wear rate to about 30  $\mu\text{m}/\text{hour}$  for a multiplier of 30/20 or 1.5. In the same way, a multiplier of 10/20 or 0.5 can be found for the decrease in solids size, and a multiplier of about 35/20 or 1.75 for the increase in volumetric solids concentration. The final estimated wear rate may then be calculated as:

$$\text{Estimated Suction Liner Wear Rate} = 20 \mu\text{m}/\text{hour} \times 1.5 \times 0.5 \times 1.75 = 26.3 \mu\text{m}/\text{hour} \quad (2)$$

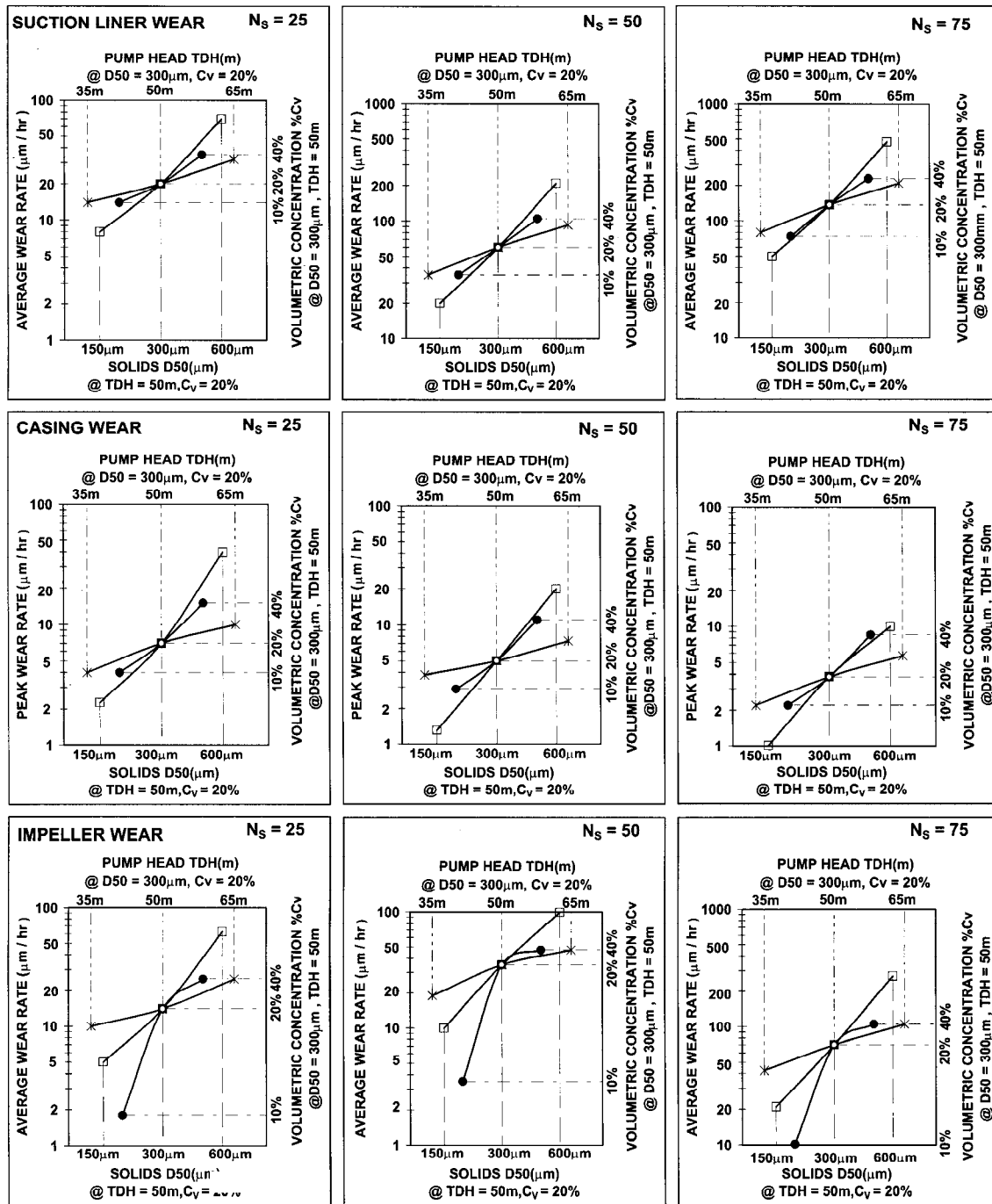


Figure 15. Summary Plot for Estimation of Slurry Pump Component Wear

The summary chart of Figure 15 gives only estimated wear rates based on the combined results of many designs. Furthermore, the basic assumptions used during the numeric simulations should be kept in mind:

- White iron slurry pump components.
- Pump operation near design flowrate.
- Silica sand slurry of typical size grading.
- Small impeller clearing vane geometries.

The chart is, however, independent of pump size and can be very useful as a first guide in estimating wear and selecting the design type best suited to the requirements of a given application. For the fine tuning of designs and troubleshooting of actual wear problems, individual numerical analyses will still be needed.

## TOTAL COST OF OWNERSHIP (TCO)

The biggest difference between a slurry pump and a water pump is of course the wear, which can account for a significant portion of the overall TCO. As a starting point in this analysis, the yearly cost of casing replacement was determined at the heavy duty condition of 50m head, 600 micron  $D_{50}$  solids and 20% volumetric concentration as seen in Figure 16.

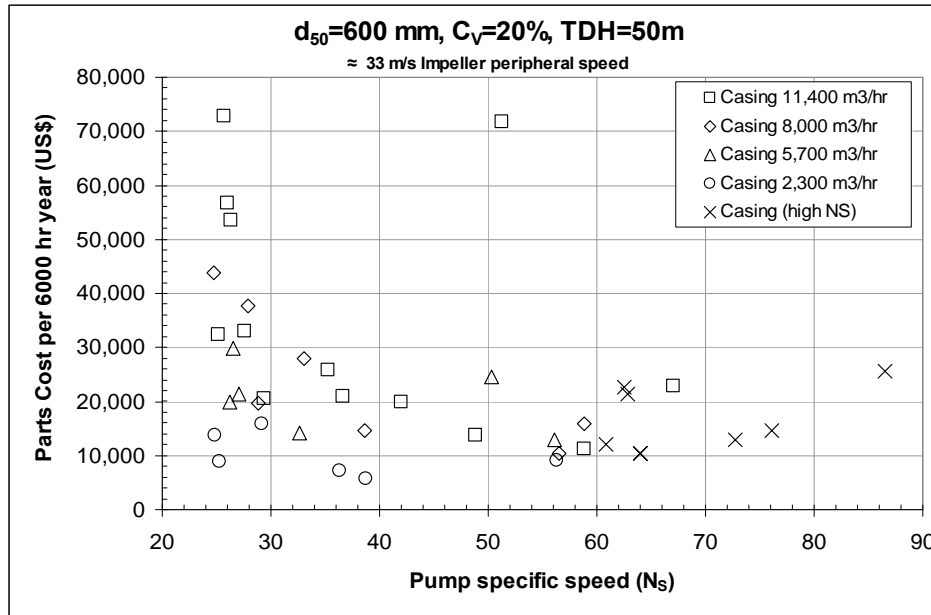


Figure 16. Yearly Casing Part Cost for Operating Condition No.7 as a function of Specific Speed.

The trend to higher casing cost at lower specific speed was expected from the results of figure 4, but is further intensified at the lowest specific speeds by the fact that the casing size (and weight) increases in the same direction as the wear. In Figure 17, the entire wet end is considered and a different picture emerges. The opposing influence of the impeller and liner wear results in a minimum parts cost at the design specific speed of  $35 N_s$  (1800 USNS).

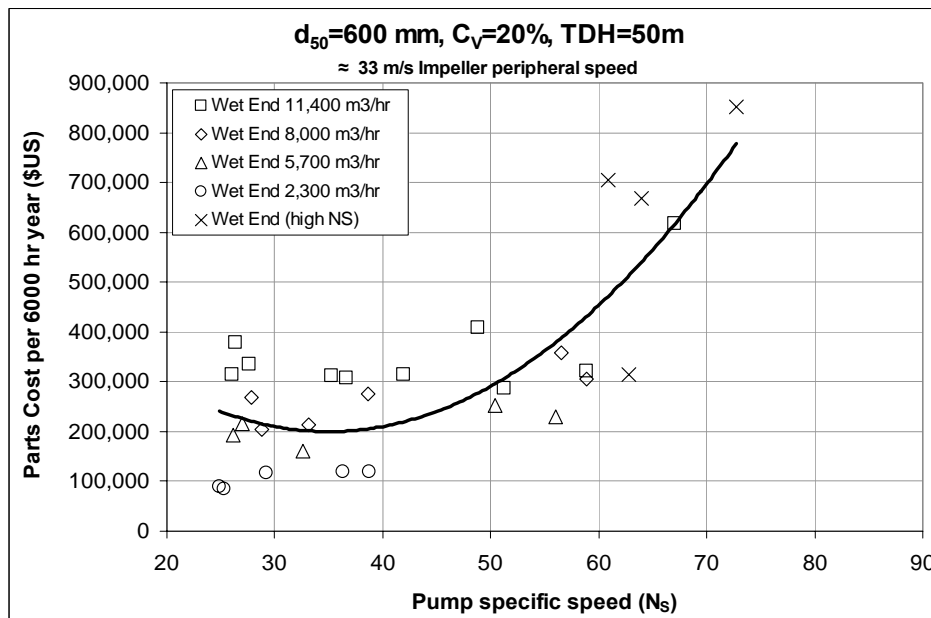


Figure 17. Yearly Wet End Parts Cost for Operating Condition No.7 as a function of Specific Speed.

In the present analysis, TCO is calculated as the sum of the energy, capital, and rebuild costs. Energy was taken to be 5¢ per kilowatt-hour and capital costs were estimated at 10% of the original pump cost per year. Rebuild costs include the wet end costs shown in figure 17, plus the periodic rebuild of the bearing assembly (estimated at 20% of the original pump cost per year at the maximum operating speed). Not included are the costs of any down time, the labor for changing out parts and the cost of the motors, any gearboxes, power supplies and buildings. The results are shown in Figure 18.

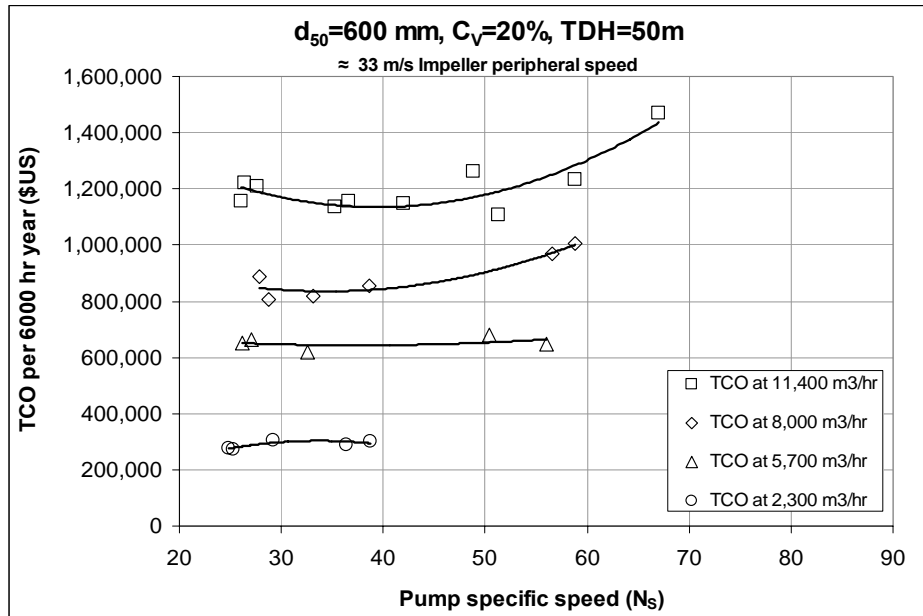


Figure 18. Yearly TCO for Operating Condition No.7 as a function of Specific Speed.

The above is, of course, only for one operating condition and the TCO may vary significantly with different conditions. Table 4 lists the calculated TCO for the large pump designs of around 11,400 m<sup>3</sup>/hr (50,000 gpm) size for a design specific speed of  $N_s = 38$  (2000 USNS) at each of the seven operating conditions considered in this study.

Case	Head m	Concentration Cv %	Solids Size D50 micron	TCO US\$ per 6,000 hour year
<b>1 (baseline)</b>	<b>50</b>	<b>20</b>	<b>300</b>	<b>960,000</b>
2	35	20	300	580,000
3	65	20	300	1,370,000
4	50	10	300	880,000
5	50	40	300	1,000,000
6	50	20	150	890,000
7	50	20	600	1,150,000

Table 4. Total Cost of Ownership at 11,400 m<sup>3</sup>/hr (50,000 gpm) and Specific Speed  $N_s = 38$  (2000 USNS)

Here it should be noted that the 35 and 65 meters cases would require more and less pumps in series respectively than the others, so the cost values should be adjusted for any comparison.

## CONCLUSION

The pump casing, suction liner and impeller components have been numerically modelled to obtain the calculated wear for different heads, solids sizes, volumetric solids concentrations and specific speed designs of pumps for white iron construction when pumping silica sand slurry.

Correlations against pump design specific speed show higher specific speed pump casings wear better, while lower specific speed, slower running, larger diameter impeller pumps have better impeller and liner wear.

Average wear plots for different specific speed pumps allowing estimation of wear rate for a wide variety of operating conditions have been produced and show that small changes in head, solids size concentration can result in large differences in component wear.

The calculated values show total cost of ownership is affected significantly by changes in operating conditions (due to wear) and is a minimum, in most cases, at around a design specific speed of  $N_s = 38$  (2000 USNS).

## REFERENCES

- Bross, S., Addie, G.R., (2001), "Prediction of Impeller Nose Wear Behaviour in Centrifugal Slurry Pumps," 4<sup>th</sup> *International Conference on Multiphase Flow*, New Orleans, LA, USA
- Kadambi, J.R., Wernet, M., Sankovic, J. and Addie, G.R. (2003), "Particulate Velocity Measurements in the Intra-Blade Passages of a Centrifugal Slurry Pump," 2003 *ASME Fluids Engineering Division Summer Meeting*, Honolulu, Hawaii, USA
- Pagalthivarthi, K.V., Desai, P.V., and Addie, G.R., (1991) "Quasi-3D Computation of Turbulent Flow in Centrifugal Pump Casings," *ASME Symposium on Multidisciplinary Application of CFD, Journal of Fluids Engineering*.
- Pagalthivarthi, K.V., Addie, G.R., (2001) "Prediction Methodology for Two Phase Flow and Erosion Wear in Slurry Impellers," 4<sup>th</sup> *International Conference on Multiphase Flow*, New Orleans, LA, USA
- Pagalthivarthi, K.V., Kadambi, J.R., and Addie, G.R., (2004), "Finite Element and PIV Studies of Particulate Flow in a Laboratory Slurry Pump Casing," *Hydrotransport International Conference*, Santiago, Chile
- Roco, M.C., (1983), "Analytical Model and Experimental Studies of Slurry Flow and Erosion in Pump Casings," *The Eighth Annual International Technical Conference on Slurry Transportation*, STA San Francisco, CA, USA
- Roco, M. C., Addie, G.R., Dennis, J., and Nair, P., (1984), "Modelling Erosion Wear in Centrifugal Slurry Pumps," 9<sup>th</sup> *International Conference on Hydraulic Transport of Solids in Pipes*, Rome, Italy
- Tian, H.H., Addie, G.R. (2003), "Experimental Study on Erosive Wear of Some Metallic Materials Using Coriolis Wear Testing Approach," *WEAR Elsevier Science B.V.*, Cambridge, UK.
- Visintainer, R.J., Addie, G. R., Pagalthivarthi, K.V., and Schiele, O.H., (1992), "Prediction of Centrifugal Slurry Pump Wear," *International Conference on Pumps and System*, Beijing, China